UCSF

Title

A tissue checkpoint regulates type 2 immunity

Permalink

https://escholarship.org/uc/item/8rc321jm

Authors

Van Dyken, Steven J
Nussbaum, Jesse C
Lee, Jinwoo
et al.

Peer reviewed

A tissue checkpoint regulates type 2 immunity

Steven J. Van Dyken[1,*], **Jesse C. Nussbaum**[1,*], **Jinwoo Lee**[1], **Ari B. Molofsky**[2], **Hong-Erh Liang**[1], **Joshua L. Pollack**[1,3], **Rachel E. Gate**[4], **Genevieve E. Haliburton**[1,5], **Chun J. Ye**[4], **Alexander Marson**[1,5,6,7], **David J. Erle**[1,3], and **Richard M. Locksley**[1,7,8]

[1]Department of Medicine, University of California San Francisco, San Francisco, CA, USA.

[2]Department of Laboratory Medicine, University of California San Francisco, San Francisco, CA, USA.

[3]Lung Biology Center, University of California San Francisco, San Francisco, CA, USA.

[4]Department of Epidemiology and Biostatistics, Institute for Human Genetics, University of California San Francisco, San Francisco, CA.

[5]Diabetes Center, University of California, San Francisco, CA.

[6]Innovative Genomics Initiative (IGI), University of California, Berkeley, CA, USA.

[7]UCSF Helen Diller Family Comprehensive Cancer Center, University of California, San Francisco, CA, USA.

[8]Howard Hughes Medical Institute, University of California San Francisco, San Francisco, CA, USA.

Abstract

Group 2 innate lymphoid cells (ILC2s) and CD4$^+$ T helper type 2 (TH2) cells are defined by their similar effector cytokines, which together mediate the features of allergic immunity. Here, we show that tissue ILC2s and TH2 cells differentiate independently but share overlapping effector function programs mediated by exposure to the tissue-derived cytokines interleukin (IL)-25, IL-33, and thymic stromal lymphopoietin (TSLP). Loss of these three tissue signals does not affect lymph node priming but abrogates terminal differentiation of effector TH2 cells and adaptive lung inflammation in a T cell-intrinsic manner. Our findings suggest how diverse perturbations activate type 2 immunity, uncovering a shared local tissue-elicited checkpoint that can be exploited to control both innate and adaptive allergic inflammation.

Pattern recognition receptors for conserved microbial structural elements and nucleic acids are critical innate sensors that shape the ensuing adaptive TH1 and TH17 responses that

protect against bacteria, fungi, and viruses. In contrast, allergy and anti-helminth immune responses, or type 2 immunity, can be elicited by a wide array of proteases, venoms, and mechanical irritants, yet our understanding of sensing pathways by which recognition of these diverse signals converges on adaptive type 2 immunity remains incomplete. The discovery of ILC2s profoundly altered the understanding of type 2 immunity. ILC2s are dispersed in peripheral tissues where they constitute the major innate sources of the cytokines IL-13 and IL-5 (ref. [1]). The ability of ILC2s to rapidly respond to epithelial cytokines such as IL-33, IL-25 and TSLP, as well as other mediators released during tissue damage[2,3], without the need for antigen specificity, has suggested models in which ILC2s instruct adaptive TH2 responses through effects on dendritic cells (DCs)[4] or direct interactions with TH2 cells[5–10]. Understanding these relationships is critical in devising strategies to attenuate type 2 immunity by therapeutically targeting shared upstream signals elicited by the wide array of allergens.

The genes encoding the type 2 cytokines IL-4, IL-13 and IL-5 share a highly conserved gene locus but exhibit divergent expression patterns in different cells and tissues during allergic inflammation[11]. Mice infected with the parasitic nematode *Nippostrongylus brasiliensis* (*Nb*), a well-established model of migratory helminth infection, develop lung inflammation accompanied by eosinophils, alternatively activated macrophages, and high concentrations of IgE[12]. The TH2 cells that drive this immune response are initially primed in the draining lymph nodes, as revealed using the 4get reporter strain: CD4+ T cells from these reporter mice express green fluorescent protein (GFP) when their *Il4* locus becomes accessible at the time of lymph node priming[13]. Most *Il4*-expressing T cells in lymph nodes are T follicular helper (TFH) cells[11], but a subset of the 4get+ lymph node T cells go on to become TH2 effector cells that migrate from the lymph node to peripheral tissues, as evidenced by their capacity to expel worms after adoptive transfer[13].

We challenged mice carrying cytokine reporter alleles with a variety of type 2 immune stimuli to dissect the regulation of type 2 immune cytokines *in vivo*. Unexpectedly, we found that activation of primed TH2 cells can occur independently of ILC2s or ILC2 cytokines, but that the effector function of both cell types is dependent on the combinatorial exposure to IL-33, IL-25, and TSLP. Because these signals were not required for lymph node priming of CD4+ T cells, we propose that they comprise a local checkpoint that restricts the differentiation of cytokine-expressing effector cells to sites of tissue damage.

RESULTS

Tissue ILC2s and TH2 cells share a core transcriptional and epigenetic profile

Using an IL-13 reporter allele (S13), we previously showed that the TH2 cells expressing IL-13, which is required for worm clearance, comprise a subset within the larger pool of 4get+ T cells[11]. Similarly, using an IL-5 reporter allele (R5)[14], IL-5-expressing TH2 cells in the lung comprise a subset of 4get+ T cells (Fig. 1a), consistent with differentiation of cytokine-expressing effector TH2 cells from primed 4get+ CD4+ T cells in lymph nodes. ILC2s, which reside and express IL-5 in peripheral non-lymphoid tissue in steady-state, accumulate in the *Nb*-infected lung prior to the arrival of IL-5-expressing TH2 cells (Fig. 1b

and Supplementary Fig. 1a), and both cell types increase their R5$^+$ percentage and the fluorescent intensity of the reporter with time (Supplementary Fig. 1b).

To assess the reliability of the reporters in accurately identifying tissue effector lymphocytes, we compared the chromatin landscape of lung ILC2s and TH2 cells by using the 4get allele to sort primed (4get$^+$) CD4$^+$ T cells from the lungs of *Nb*-infected mice and to analyze them along with rigorously gated lung ILC2s using the Assay for Transposase-Accessible Chromatin using Sequencing (ATAC-Seq)[15]. As a control population, we also analyzed primed (4get$^+$) CD4$^+$ T cells in the lung-draining lymph nodes that had not migrated to the lung. Regardless of their tissue of origin, when analyzed across the entire genome, 4get$^+$ T cells exhibited chromatin accessibility that was different from that of ILC2s, including differences at expected loci such as *Cd4*, *Arg1*, and *Il4* (Supplementary Fig. 2a, b)[16]. Consistent with the cytokine reporter data, lung 4get$^+$ T cells diverged from lymph node 4get$^+$ T cells at loci associated with effector function, including *Il5* and *Il13* (Fig. 1c). Further, when we compared these populations at regions previously identified as T effector cell-specific "super-enhancers"[17], lung 4get$^+$ TH2 cells more closely resembled ILC2s than lymph node T cells, with Pearson correlation coefficients of 0.79 and 0.67, respectively (Supplementary Fig. 2c). Peaks in specific genes associated with effector function, including *Gata3* and *Rora*, indicated increased chromatin accessibility within these loci among lung tissue ILC2 and T cell effector populations, in contrast to the primed 4get$^+$ T cells in lymph nodes (Fig. 1c). Thus, although the *Il4* locus was primed in all lymph node 4get$^+$ T cells, and although this pool includes cells with TH2 effector potential[10], chromatin accessibility at the *Il5* and *Il13* loci was only enriched among 4get$^+$ T cells that had exited the lymph node and entered the inflamed tissue.

The epigenetic similarities between lung ILC2s and tissue effector TH2 cells suggested that chromatin accessibility in these tissue-resident cells directs a shared gene expression program. To test this hypothesis, we used the IL-5 reporter allele to isolate actively cytokine-expressing TH2 cells from the lungs of *Nb*-infected mice and compared their transcriptional profile to IL-5-expressing ILC2s by RNA sequencing (RNA-Seq) (Fig. 1d, Supplementary Fig. 2d, Supplementary Tables 1–3). As assessed in this way, ILC2s and tissue effector TH2 cells shared expression of cell surface receptors and cytokines, suggesting that they sense and respond similarly to the tissue microenvironment. Indeed, many transcription factors important for ILC2 differentiation and/or function[18] were comparably expressed in tissue effector TH2 cells.

IL-5-mediated deletion attenuates type 2 immunity in non-lymphoid tissue

The transcriptional and epigenetic similarities we observed between these cytokine-competent tissue-localized lymphocyte effectors, including their high expression of *Rora*, suggested that prior ILC2 deletion strategies[4–6,19,20] might be complicated by potential cell-intrinsic effects on tissue TH2 effector cells. In addition, reconstitution strategies in other models of ILC2 deficiency, such as common γ cytokine receptor chain (γ$_C$) or the IL-7 receptor α chain (*Il7ra*), are limited by aberrant lymph node development that precludes accurate assessments of TH2 differentiation[21].

In R5 reporter mice, the only R5+ cells after *Nb* infection are ILC2s and TH2 cells (Supplementary Fig. 3a), and, as previously shown using dual IL-5/IL-13 reporter mice[11], all of the IL-13-expressing ILC2s are contained within the R5hi subset (Fig 2a). Based on this finding, we crossed R5/R5 mice, whose cells carry a *Cre* element in the *Il5* gene, to mice carrying a ROSA26-flox stop-diphtheria toxin A "Deleter" allele[22] to delete activated effector cells. In R5 Deleter mice, 90% of lung ILC2s, which constitutively express IL-5, were deleted at rest (Supplementary Fig. 3b)[14], and 5 and 10 days after *Nb* infection, worm clearance, ILC2 accumulation, and IL-13-mediated eosinophil recruitment were impaired (Fig. 2b–d). As expected, deletion of cytokine-expressing effector cells resulted in diminished total lung T cells as well as the percent that were R5+ TH2 effector cells (Fig. 2e).

Despite the loss of ILC2s, however, CD4+ T cells in the lymph node made up a similar percentage of total cells, the fraction of these CD4+ cells that were CXCR5+PD-1+ TFH cells was normal, and serum IgE responses were elevated in comparison to mice lacking the Deleter allele (Fig. 2f, g and Supplementary Fig. 3c). Thus, IL-5-mediated deletion impacts tissue, but not lymph node, immunity, consistent with IL-5 expression by IL-13-producing resident ILC2s and the infiltrating newly differentiating TH2 effector cells.

Activation of adaptive type 2 immunity despite ILC2 deficiency

To further assess the contribution of ILC2s to tissue TH2 cell recruitment and IL-13-dependent worm clearance, we crossed R5/R5 and R5/R5 Deleter mice onto Rag1-deficient backgrounds and reconstituted them with naïve CD4+ T cells from R5/+ heterozygous mice (Supplementary Fig. 3d). Rag1-deficient mice failed to clear worms by 10 days after infection, whereas reconstituted mice cleared the infection, regardless of whether they carried the Deleter allele (Fig. 3a). Despite substantial ILC2 deletion (Fig. 3b), the capacity of transferred cells to migrate to the lung and become tissue effector TH2 cells was unimpaired, and eosinophil recruitment was normal (Fig. 3c). We also tested the role of ILC2 expression of MHCII by crossing the R5/+ mice with mice carrying a "floxed" allele of the *H2-Ab1* gene. Although ILC2s from these mice demonstrated loss of MHCII expression (Supplementary Fig. 3e), there were no differences in the numbers of lung ILC2s, eosinophils, CD4+ T cells, or R5+ TH2 effector cells (Fig. 3d–f). These findings are consistent with those using an IL-13-driven Deleter allele[11] and suggest that ILC2s are not required for TFH function, TH2 cell priming in the lymph nodes, and acquisition of TH2 tissue effector function in tissue.

Multiple tissue cytokines are required for local type 2 inflammation

Our data raised the possibility that local signals drive terminal differentiation of both innate and adaptive lymphocytes. The epithelial cytokines TSLP, IL-25, and IL-33 mediate ILC2 activation[23] and have also been implicated in TH2 cell function[24–26]. In confirmation of the RNA-sequencing data, the surface expression of IL-33-receptor (IL-33R) and TSLP-receptor (TSLPR) was comparable on R5+ ILC2s and R5+ TH2 cells (Fig. 4a). Although undetectable in serum, TSLP, IL-25, and IL-33 proteins were elevated in the lung after *Nb* infection (Fig. 4b and data not shown), corresponding with increased ILC2s and tissue effector TH2 cells that persisted in the lung for weeks after infection (Fig. 4c).

The presence of multiple cytokines in the inflamed tissues, coincident with the expansion of the ILC2 and TH2 cell compartments, suggested potentially additive or synergistic signals that regulate type 2 immunity. We crossed mice triply-deficient in TLSPR, IL-33R, and IL-25 cytokine ("TKO")[23] onto 4get[13] and Arg1-YFP[16] backgrounds to assess TH2 priming, ILC2s, and alternatively activated macrophages (AAMs). After infection, TKO mice on both BALB/c and C57BL/6 backgrounds showed > 90% reductions in lung eosinophils and AAMs, decreased ILC2s, and delayed worm clearance; deficits were more severe than those in single- and double-deficient animals (Fig. 4d–f and Supplementary Fig. 4a–d)[27,28]. Total lung CD4$^+$ T cells, however, were not statistically different in TKO animals, and the percentage of 4get$^+$ primed TH2 cells in the lung tissue was only partially diminished (Fig. 4g, h). Similar results were observed after intranasal challenge with fungal or house dust mite (HDM) extracts; in both, the numbers of 4get$^+$ lymph node T cells and serum IgE were unaffected (Supplementary Fig. 4e–g), the numbers of 4get$^+$ lung T cells was partially decreased (Supplementary Fig. 4h, i), but the tissue type 2 immune response as assessed by lung eosinophils and AAMs was almost completely abrogated on both BALB/c (Supplementary Fig. 4j, k) and C57BL/6 backgrounds (Supplementary Fig. 4l, m). Tissue neutrophil infiltration in response to HDM extract was unaffected, however (Supplementary Fig. 4n), indicating specific abrogation of type 2 tissue effects in TKO mice.

Tissue cytokines are not required for lymph node priming of adaptive immunity

In contrast to lung ILC2s and TH2 cells, lymph node 4get$^+$ T cells expressed low amounts of IL33R and TSLPR (Fig. 5a), and, consistent with a role for IL-33, TSLP, and IL-25 in tissue responses rather than in lymph node priming, early dendritic cell (DC) subsets in the draining lymph node were normal in TKO mice (Fig. 5b), as were subsequent serum IgE, B cell and CD4$^+$ T cell numbers, and the percentage of activated (CD25$^+$CD62L$^−$) and primed (CD44$^+$4get$^+$) CD4$^+$ T cells (Fig. 5c–e and Supplementary Fig. 5a).

Similar results were observed after intranasal challenge with fungal or HDM extracts (Supplementary Fig. 4e–n), and further evidence of this paradigm was borne out in a tissue site other than the lung. A bee venom toxin, the cytolytic enzyme phospholipase A2 (bvPLA2), induces IL-33-dependent ILC2 activation and an allergic immune response.[29] After intraperitoneal toxin administration, lymph node responses and IgE induction, along with 4get$^+$ CD4$^+$ T cell tissue infiltration, were unimpaired in TKO mice (Supplementary Fig. 5b–d), whereas peritoneal eosinophilia was substantially compromised as compared to wild-type mice, and more so in TKO as compared to ST2-deficient mice (Supplementary Fig. 5e). Taken together, these data demonstrate in diverse tissue sites and disparate models of allergic inflammation that, although epithelial cytokines are critical for local type 2 tissue immune responses, they are not essential for the afferent processes that prime allergic immunity in draining lymph nodes.

To define the anatomic location of TH2 effector cell terminal differentiation, we administered FTY720 to mice 2, 4, and 6 days after *Nb* infection to block egress of lymphocytes into the circulation during priming[30] and analyzed the results on day 7. Treatment with FTY720 caused profound lymphopenia in the peripheral circulation and lung (Supplementary Fig. 5f), but an increase in the percentage of lung TH2 effector cells (Fig.

5f), indicating effective blockade of circulation and/or increased availability of instructive signals to the small pool of primed T cells able to reach the lung. Although lymph node egress was blocked, however, there was no accumulation of R5[+] or S13^{+} T cells in the draining lymph node (Fig. 5f and Supplementary Fig. 5g), consistent with a lack of signals capable of mediating acquisition of full TH2 cell IL-5 and IL-13 production in lymph nodes.

Tissue cytokine licensing of TH2 cells is cell-intrinsic

In all of these type 2 immune challenges, primed 4get^{+} TH2 cells reached the lungs in TKO mice but failed to gain cytokine-secreting potential, suggesting a localized deficit in terminal differentiation. To determine the functional consequence of epithelial cytokine signaling on ILC2s and primed TH2 cells, we purified these cells from the lungs of infected mice and cultured them separately in IL-7 or IL-7 plus ionomycin and phorbol 12-myristate 13-acetate (Ion/PMA). *Nb*-activated ILC2s and primed 4get^{+} TH2 cells from the lungs of TKO mice had markedly attenuated IL-5 and IL-13 production under both culture conditions as compared to cells collected from wild-type mice (Fig. 6a and Supplementary Fig. 6a). In corroboration of these *in vitro* culture results, TKO lung CD4^{+} T cells and ILC2s analyzed immediately *ex vivo* after *Nb* infection or HDM challenge exhibited markedly decreased R5 and S13 reporter expression as compared to wild-type cells (Supplementary Fig. 6b–e). Similar deficits were observed among peritoneal CD4^{+} T cells after bvPLA2 challenge (Supplementary Fig. 7a). The inability of TKO T cells to secrete type 2 cytokines was not due to a developmental defect, however, as *in vitro* culture of naïve TKO CD4^{+} T cells resulted in normal TH2 polarization and cytokine production (Supplementary Fig. 7b, c). In contrast, although adoptively transferred naïve CD4^{+} T cells lacking TSLPR and IL33R (DKO) were primed and accumulated normally in lung tissue in both wild-type and IL25 KO recipients (to recreate TKO conditions) after *Nb* infection, sorted 4get^{+} CD4^{+} T cells from DKO donors produced significantly less IL-5 and IL-13 than similarly transferred and primed wild-type T cells (Fig. 6b).

When equal numbers of congenically marked wild-type and TKO CD4^{+} T cells from 4get donors were transferred into Rag1-deficient mice before *Nb* infection, we observed equal expansion of wild-type and TKO total T cells and primed 4get^{+} TH2 cells in the lungs of recipient mice (Fig. 6c). The primed TKO 4get^{+} TH2 cells, however, produced significantly less IL-5 and IL-13 than wild-type 4get^{+} TH2 cells after culture *ex vivo* in either IL-7 or Ion/PMA (Fig. 6d). We observed comparable results when wild-type or TKO cells were transferred into Rag1-deficient mice before intranasal administration of the protease allergen papain[7,8] (Supplementary Fig. 7d–g).

Together, these data suggest that optimal TH2 effector function requires local epithelial cytokine signaling in a cell-intrinsic manner in response to a broad array of type 2 immune challenges that share the capacity for local tissue perturbation. To assess this using CD4^{+} T cells differentiating side-by-side within an intact immune system, we adoptively transferred wild-type congenically marked naïve T cells into wild-type and TKO mice before infecting the recipients with *Nb*. As before, host ILC2s and primed TH2 cells cultured from wild-type, but not TKO, lungs secreted IL-5 and IL-13 (Fig. 7a). In contrast, the transferred wild-type T cells secreted equivalent amounts of IL-5 and IL-13 (Fig. 7b) and mediated worm clearance

(Supplementary Fig. 7h) regardless of whether their priming occurred in wild-type or TKO hosts. Thus, primed T cells intrinsically capable of sensing locally-elicited tissue cytokines develop into effector TH2 cells, even in a microenvironment in which resident dendritic cells, as well as host ILC2s and TH2 cells unable to sense local cytokines fail to generate type 2 effector cytokines.

DISCUSSION

Taken together, our data suggest a model whereby naïve CD4^{+} T cells are primed in draining lymph nodes and migrate into inflamed tissues, at which point TH2 cell effector differentiation is completed in response to combinatorial cytokine signals derived from the local microenvironment. These same cytokine signals also mediate ILC2 function[18], but ILC2s themselves are neither required for adaptive immune responses in the draining lymph nodes nor for tissue effector TH2 cell differentiation; rather, both ILC2s and TH2 cells are subject to a lymphocyte-intrinsic checkpoint that restricts type 2 cytokines to sites of tissue distress. Such a model may explain how type 2 immunity can be activated by diverse tissue perturbations, including proteases, venoms, chitin aggregates, or mechanical injury, that do not share microbial-associated molecular patterns implicated in TH1- and TH17-mediated host immunity. These findings validate the strategy of blockade of tissue signals for treating allergic disease[31], and further study will be needed to assess whether blockade of multiple pathways may prove a more efficacious approach than targeting any single cytokine or receptor.

Although emerging transcriptional profiles of innate and adaptive lymphocytes subsets allow comparison of various subsets [32–34], our approach relies on isolation of cells from tissues based on genetically-encoded function marking of cytokine genes. Although nearly all lung ILC2s are constitutively positive for IL-5, only a proportion of these cells become IL-13-secreting cells after allergic challenges. Among lung-infiltrating CD4^{+} T cells after migratory helminth infection, only a small proportion constitute the IL-13- and IL-5-secreting effector cells that mediate immunity[11]. By focusing on these tissue effector TH2 cells, we uncovered the substantial overlap between the chromatin landscape and the transcriptionally active components of ILC2s and tissue effector TH2 cells. The shared transcription factor programs expressed by these cells suggest comparable abilities to interrogate and interact with their tissue microenvironment, in contrast with T cells that are undergoing priming in the lymph node. Although prior studies have implicated epithelial cytokines in type 2 immunity[23–29,35,36], we show that IL-25, IL-33, and TSLP represent a shared means for ILC2 and TH2 cells to independently acquire terminal effector function in lung tissue, thereby comprising a checkpoint for effector cytokine acquisition. We found additional evidence for this checkpoint in peritoneum; however, separate or additional signals may mediate this acquisition across diverse tissue compartments, where tissue-specific programs exist for other ILC subsets[37] and their T-helper cell counterparts.

Recent evidence suggests that tissue ILC2s are present in tissues at birth and expand to reach adult levels around the time of weaning[14]. In response to tissue perturbations, ILC2s activate and expand locally without exchange from blood-borne precursors, as demonstrated using parabiosis[38]. As previously shown[23], ILC2 numbers in lung are normal in TKO mice, but, as

shown here in the context of adaptive immune challenges, fail to express their canonical cytokines, IL-5 and IL-13. Future study will be needed to elucidate the molecular pathways by which these cells, like the 4get^{+} primed CD4^{+} T cells that accumulate in the lungs of TKO mice challenged with allergens, fail to achieve terminal effector cell differentiation. We speculate that ILC2s, which assume their position in tissues and activate cytokine expression in response to local tissue perturbations in the post-birth environment, initiate this transition in a manner similar to what is later re-visited by adaptive TH2 cells arriving in peripheral tissues after priming in draining lymph nodes in response to immune challenges.

Whether some tissue effector TH2 cells persist as long-lived tissue resident effectors alongside developmentally positioned innate cells requires further study, but our findings, here demonstrated primarily in the lung, will likely be extended to other T cell subsets and tissues with their own tissue-specific combinations of checkpoint signals[39–41]. Further studies of the nature and components of these checkpoints may have great therapeutic potential, not only for reducing allergic pathology, but also for enhancing beneficial homeostatic pathways associated with these responses.[42]

ONLINE METHODS

Mice

Single, double, and triple-deficient $Crlf2^{-/-} Il25^{-/-} Il1rl1^{-/-}$ (TKO) mice[23] carrying $Il4^{4get\ 13}$, $Arg1^{Yarg\ 43}$, $Il13^{Smart/Smart\ 11}$, and $Il5^{Red5\ 14}$ reporter alleles on both BALB/c and C57BL/6J backgrounds were analyzed in comparison to age- and sex-matched wild-type (WT) control mice derived from the same breeding schemes. Additional mice included $Gt(Rosa)26^{DTA/DTA\ 22}$, and BALB/c CD45.1 (CBy.SJL(B6)-$Ptprc^a$/J; 006584), C57BL/6J CD45.1 (B6.SJL-$Ptprc^a\ Pep c^b$/BoyJ; 002014), C57BL/6J and BALB/c $Rag1^{-/-}$ [B6.129S7-$Rag1^{tm1Mom}$/J; 002216; C.129S7(B6)-$Rag1^{tm1Mom}$/J; 003145], and MHCII-flox (B6.129×1-$H2$-$Ab1^{tm1Koni}$/J; 013181) were obtained from The Jackson Laboratory. Mice were maintained under specific pathogen-free conditions. All procedures were approved by the UCSF IACUC.

In vivo treatments

Mice were infected subcutaneously with 500 *N. brasiliensis* third-stage larvae (L3), with infection and maintenance procedures as described. For adoptive transfer, naïve CD4^{+} T cells were isolated from pooled lymph nodes and enriched to >98% purity by negative magnetic selection (Thermo Fisher Dynabeads or Miltenyi Biotec). Recipient C57BL/6J Rag1-deficient mice were given 10^7 donor R5/+ T cells intravenously in 250 mL sterile phosphate-buffered saline (PBS; Ca^{++}, Mg^{++} free) and were allowed to engraft for 7 days before *N. brasiliensis* infection, then euthanized at 10 d.p.i. for analysis. For mixed T cell transfers (Fig. 6c, d), 2.5×10^6 naïve CD4^{+} T cells from WT 4get CD45.1/2 and TKO 4get CD45.2 BALB/c donor mice were mixed 1:1 and allowed to engraft for 15 days after transfer into Rag1-deficient BALB/c recipients, which were infected with *N. brasiliensis* and euthanized at 8 d.p.i. for analysis. Recipient WT, IL-25 KO, or TKO mice were irradiated sublethally (450 rads) 1 day before intravenous transfer of 2×10^6 donor T cells in 200 μl sterile PBS, and adoptively transferred CD4^{+} T cells were allowed to engraft for 18 (Fig. 6b)

or 45 (Fig. 7) days before recipient mice were infected, then euthanized at indicated time points for cell preparation and analysis.

Intranasal challenges with house dust mite enriched for fecal pellets (HDM; 318 fecal pellets : 28 mite bodies : 19 egg castings from *Dermatophagoides farinae*; Greer) or *Aspergillus niger* hyphal preparation were prepared and administered as previously described[44], 3 times weekly for 3 weeks, followed by analysis 48 hours after the final dose. Mice were injected intraperitoneally with 50 μg phospholipase A2 from bee venom (*Apis mellifera*; Sigma) on days 0, 7, and 13, then euthanized on day 14 for collection of serum, lymphoid tissues, and peritoneal exudate cells (PEC). For papain challenge (Supplementary Fig. 7), 2.5×10^6 naïve $CD4^+$ T cells from WT 4get and TKO 4get BALB/c donor mice were allowed to engraft for 15 days after transfer into Rag1-deficient BALB/c recipients, which received 4 doses of 30 μg papain (from *Carica papaya*; Sigma) intranasally on days 0, 3, 7, and 9, then were euthanized on day 10 for cell preparation and analysis. FTY720 (Sigma) was dissolved in methanol for a stock solution of 5 mg/ml and this was further diluted 1 : 40 in normal saline prior to treatment. Mice received 25 μg in 200 μl (1 mg/kg) intraperitoneally on days 2, 4, and 6 post infection.[30] Vehicle-treated control mice received 200 μl of 2.5% methanol in normal saline.

Tissue preparation and cell sorting

Single-cell suspensions from peripheral blood, lung, lymph nodes, spleen, and peritoneal cavity were prepared for flow cytometry as previously described[14,23,29], using the following antibodies: phycoerythrin (PE)/cyanine (Cy)7- or Pacific Blue (PB)-anti-CD11c (N418), Brilliant Violet (BV) 650-, PB-, or allophycocyanin (APC)-anti-CD11b (M1/70), PB- or peridinin chlorophyll protein complex (PerCP)/Cy5.5-anti-Gr-1 (RB6–8C5), APC- or APC/Cy7-anti-Ly6G (1A8), eFluor450-anti-F4/80 (BM8), PB- or PerCP/Cy5.5-anti-CD3 (17A2), PB-, BV711-, BV605- or APC/Cy7-anti-CD4 (RM4–5), PE/Cy7-anti-CD5 (53–7.3), PB- or APC/eFluor780-anti-CD8α (53–6.7), PB-anti-CD19 (6D5), APC- or APC/Cy7-anti-CD25 (PC61), PE/Cy7-anti-CD45.1 (A20), Qdot650- or APC/eFluor780 anti-CD45.2 (104), APC/eFluor780-anti-CD45R (B220), eFluor450- or APC-anti-CD49b (DX5), PerCP/Cy5.5-anti-CD127 (A7R34), PB-, PE/Cy7- or APC-anti-NK1.1 (PK136), PE/Cy7-anti-NKp46 (29A1.4), APC- or BV605-anti-Thy1.2 (53–2.1), PE- or APC-anti-human CD4 (RPA-T4), streptavidin-FITC, APC-, PE/Cy7- or PerCP/eFluor710-anti-KLRG (2F1), APC-anti-IL-17RB (752101), FITC-anti-TSLPR (polyclonal; R&D Systems), biotin-anti-T1/ST2 (DJ8; MD Biosciences), APC-anti-SiglecF (E50–244), Alexa Flour 488-anti-I-A/I-E (M5/114.15.2), and APC-CD1d tetramers (PBS-57-loaded and unloaded) were obtained from the National Institutes of Health tetramer core facility. An Alexa Fluor 488-conjugated anti-SiglecF antibody was generated using purified anti-SiglecF (E50–2440, BD Pharmingen) with an Alexa Fluor 488 Monoclonal Antibody Labeling Kit (Life Technologies). Exclusion of DAPI (4',6-diamidine-2'-phenylindole dihydrochloride; Roche) identified live cells, which were enumerated with flow cytometric counting beads (CountBright Absolute; Life Technologies). Sample data were acquired using BD FACSDiva with a 4-laser LSRII or Fortessa flow cytometer (BD Biosciences) and analyzed using FlowJo software (Tree Star, Inc.). $CD4^+$ $Thy1.2^+$ T cells ($CD45.1^+$, $CD45.2^+$ and/or $4get^+$ where indicated) and $CD25^+$ $Arg1^+$ $Thy1.2^+$ ILC2s (negative for PBS-57-loaded-CD1d

tetramer, CD8α, CD11b, CD11c, CD19, DX5, NK1.1, F4/80, Ter119, Gr-1) were sorted to >95% purity using a MoFlo XDP (Beckman Coulter).

In vitro cell cultures

Sorted cells were cultured (37°C, 5% CO_2) at 5000 cells/well for 24 hrs in 100 μl RPMI-1640 containing 10% heat-inactivated FBS, penicillin-streptomycin-L-glutamine (1X), and 2-mercaptoethanol (Life Technologies), plus IL-7 (10 ng/ml; R&D Systems), or where indicated, ionomycin (Ion; 500 ng/ml) and phorbol 12-myristate 13-acetate (PMA; 40 ng/ml; Sigma). After centrifugation, cell-free supernatants were collected for protein analysis, while cells were resuspended and stained for flow cytometric analysis.

ATAC-Sequencing

Cells from 4get and 4get TKO (BALB/c) mice were sorted as above and subjected to Assay for Transposase-Accessible Chromatin using Sequencing (ATAC-Seq) through a modified version of the original protocol[15]: briefly, 50,000 – 75,000 cells were sorted into PBS, washed once, and then lysed in 100 μl of mild detergent (100 mM Tris-HCl pH 7.4, 10 mM NaCl, 3 mM $MgCl_2$, 0.1% IGEPAL CA-630) on ice for 5 minutes to release the nuclei. Pelleted nuclei were then incubated for 90 minutes with Tagment DNA Enzyme transposase from the Nextera DNA Library Preparation kit (Illumina). The reaction was stopped and DNA was purified using the MinElute Reaction Cleanup kit (Qiagen). The eluted DNA was amplified with the NEBNext High-Fidelity 2x PCR Master Mix using Nextera index primers (Illumina). The indexed libraries were purified using the MinElute PCR Reaction Cleanup (Qiagen) before sequencing on an Illumina HiSeq 2500 with 25 bp paired-end reads. Sequenced reads were aligned to mm9 using the Burrows-Wheeler Aligner algorithm[45]. Reads aligning to centromeres, telomeres, and mitochondrial DNA were filtered out using BEDtools[46], and duplicate reads were removed using Picard Tools[47]. The filtered reads were then concatenated according to cell and tissue type, and differential peaks were called using MACS2[48]. Additional comparisons were made on peaks that were found to intersect with a list of 1,328 previously published T cell specific super enhancers[17].

RNA-Sequencing

R5^{+} CD90.2^{+}CD4^{+}CD5^{+} cells and R5^{+} CD90.2^{+}CD4^{−}CD5^{−} cells were sorted from the lungs of 4 R5/+ reporter (C57BL/6J) mice 14 days after infection with *N. brasiliensis* into RLT media and immediately processed using the RNEasy Micro Plus kit (Qiagen). This was repeated with 3 mice, and 1 sample from each population was excluded due to handling error, for a total n = 6 TH2 and n = 6 ILC2 samples, with at least 5,000 cells per sample. Total RNA quality was assessed by NanoDrop spectrophotometer (Thermo Fisher Scientific) and the Agilent 2100 Bioanalyzer (Agilent Technologies). RNA sequencing libraries were generated using the NuGen Ovation RNA-Seq System V2 and the Ultralow Library System V2 kits, according to the manufacturer's protocol (NuGen Technologies). Library fragment size distributions were assessed using the Bioanalyzer 2100 and the DNA high-sensitivity chip. Library concentrations were measured using KAPA Library Quantification Kits (Kapa Biosystems), and equal amounts of indexed libraries were pooled and sequenced on HiSeq 2500 machines (Illumina) from which we obtained 574 million reads with an average per/ sample depth of 35.9 million. One T cell sample was excluded due to low unique mappable

reads resulting in n = 6 and n = 5 analyzed biological replicates of ILC2s and TH2 cells, respectively. Sequence alignment and splice junction estimation was performed using the software programs Bowtie2[49] and TopHat[50] respectively. Mappings were restricted to those that were uniquely assigned to the mouse transcriptome, as provided by Ensembl[51] and aggregated on a per-gene basis. We analyzed this raw data using DESeq[52] to assess differential expression.

In vitro CD4+ T cell polarization

CD4+ T cells were isolated from the lymph nodes of mice using negative selection (Thermo Fisher Dynabeads) and cultured in plates pre-coated with anti-CD3ε and anti-CD28 (BD Pharmingen) under standard TH2 polarization conditions for four days, as described[14]. On day 5 the supernatants were removed for cytokine measurement and the cells were washed and analyzed for 4get (GFP) allele expression.

Cytokine and IgE quantification

Supernatants from cell cultures (see above) were assayed using IL-5 and IL-13 Flex Sets with Cytometric Bead Array kit (BD). Bead fluorescence was captured on an LSRII (BD) and analyzed using Flow Cytometric Analysis Program (FCAP) Array software (BD). Blood was collected in serum separator tubes (BD) and centrifuged at 10,000 g for 10 minutes to isolate serum, which was assayed for IgE by ELISA MAX Standard IgE set (Biolegend). For lung cytokine measurements, the whole lung was homogenized, lysates were normalized to equal protein-containing volumes, and cytokine abundance was measured by ELISA as described[23].

Statistical analysis

Results from independent experiments were pooled whenever possible, and all data were analyzed using Prism (GraphPad Software). Statistical analysis for RNA-Seq data is described above. Otherwise, all data were analyzed by comparison of means using unpaired two-tailed Student's t tests. If the groups to be compared had significantly different variances ($P < 0.05$ by F test) then Welch's correction was performed. Data in all figures represent mean ± SEM unless otherwise indicated.

Accession codes

RNA-Seq data and ATAC-Seq data have been deposited in NCBI's GENE Expression Omnibus and are accessible through GEO Series accession numbers GSE70020 and GSE79703, respectively.

Supplementary Material

Refer to Web version on PubMed Central for supplementary material.

Acknowledgments

REFERENCES

1. Spits H, et al. Innate lymphoid cells--a proposal for uniform nomenclature. Nat Rev Immunol. 2013; 13:145–149. [PubMed: 23348417]

2. Patel N, et al. A2B adenosine receptor induces protective antihelminth type 2 immune responses. Cell Host Microbe. 2014; 15:339–350. [PubMed: 24629340]

3. Doherty TA, et al. Lung type 2 innate lymphoid cells express cysteinyl leukotriene receptor 1, which regulates Th2 cytokine production. J Allergy Clin Immunol. 2013; 132:205–213. [PubMed: 23688412]

4. Halim TY, et al. Group 2 innate lymphoid cells license dendritic cells to potentiate memory Th2 cell responses. Nat Immunol. 2015

5. Oliphant CJ, et al. MHCII-mediated dialog between group 2 innate lymphoid cells and CD4(+) T cells potentiates type 2 immunity and promotes parasitic helminth expulsion. Immunity. 2014; 41:283–295. [PubMed: 25088770]

6. Pelly VS, et al. IL-4-producing ILC2s are required for the differentiation of Th2 cells following Heligmosomoides polygyrus infection. Mucosal Immunol. 2016

7. Mirchandani AS, et al. Type 2 innate lymphoid cells drive CD4^{+} Th2 cell responses. J Immunol. 2014; 192:2442–2448. [PubMed: 24470502]

8. Drake LY, Iijima K, Kita H. Group 2 innate lymphoid cells and CD4^{+} T cells cooperate to mediate type 2 immune response in mice. Allergy. 2014; 69:1300–1307. [PubMed: 24939388]

9. Gold MJ, et al. Group 2 innate lymphoid cells facilitate sensitization to local, but not systemic, Th2-inducing allergen exposures. J Allergy Clin Immunol. 2014; 133:1142–1148. [PubMed: 24679471]

10. Liu B, Lee JB, Chen CY, Hershey GK, Wang YH. Collaborative interactions between type 2 innate lymphoid cells and antigen-specific CD4^{+} Th2 cells exacerbate murine allergic airway diseases with prominent eosinophilia. J Immunol. 2015; 194:3583–3593. [PubMed: 25780046]

11. Liang HE, et al. Divergent expression patterns of IL-4 and IL-13 define unique functions in allergic immunity. Nat Immunol. 2012; 13:58–66.

12. Finkelman FD, et al. Interleukin-4- and interleukin-13-mediated host protection against intestinal nematode parasites. Immunol Rev. 2004; 201:139–155. [PubMed: 15361238]

13. Mohrs M, Shinkai K, Mohrs K, Locksley RM. Analysis of type 2 immunity in vivo with a bicistronic IL-4 reporter. Immunity. 2001; 15:303–311. [PubMed: 11520464]

14. Nussbaum JC, et al. Type 2 innate lymphoid cells control eosinophil homeostasis. Nature. 2013; 502:245–248. [PubMed: 24037376]

15. Buenrostro JD, Giresi PG, Zaba LC, Chang HY, Greenleaf WJ. Transposition of native chromatin for fast and sensitive epigenomic profiling of open chromatin, DNA-binding proteins and nucleosome position. Nat Methods. 2013; 10:1213–1218. [PubMed: 24097267]

16. Bando JK, Liang HE, Locksley RM. Identification and distribution of developing innate lymphoid cells in the fetal mouse intestine. Nat Immunol. 2015; 16:153–160. [PubMed: 25501629]

17. Vahedi G, et al. Super-enhancers delineate disease-associated regulatory nodes in T cells. Nature. 2015; 520:558–562. [PubMed: 25686607]

18. Sonnenberg GF, Artis D. Innate lymphoid cells in the initiation, regulation and resolution of inflammation. Nat Med. 2015; 21:698–708. [PubMed: 26121198]

19. Halim TY, et al. Group 2 innate lymphoid cells are critical for the initiation of adaptive T helper 2 cell-mediated allergic lung inflammation. Immunity. 2014; 40:425–435. [PubMed: 24613091]

20. Wong SH, et al. Transcription factor RORα is critical for nuocyte development. Nat Immunol. 2012; 13:229–236. [PubMed: 22267218]

21. Mebius RE. Organogenesis of lymphoid tissues. Nat Rev Immunol. 2003; 3:292–303. [PubMed: 12669020]

22. Voehringer D, Liang HE, Locksley RM. Homeostasis and effector function of lymphopenia-induced "memory-like" T cells in constitutively T cell-depleted mice. J Immunol. 2008; 180:4742–4753. [PubMed: 18354198]

23. Van Dyken SJ, et al. Chitin activates parallel immune modules that direct distinct inflammatory responses via innate lymphoid type 2 and γδ T cells. Immunity. 2014; 40:414–424. [PubMed: 24631157]

24. Wang YH, et al. IL-25 augments type 2 immune responses by enhancing the expansion and functions of TSLP-DC-activated Th2 memory cells. J Exp Med. 2007; 204:1837–1847. [PubMed: 17635955]

25. Wang Q, Du J, Zhu J, Yang X, Zhou B. Thymic stromal lymphopoietin signaling in CD4(+) T cells is required for Th2 memory. J Allergy Clin Immunol. 2015; 135:781–791. e783. [PubMed: 25441291]

26. Endo Y, et al. The interleukin-33-p38 kinase axis confers memory T helper 2 cell pathogenicity in the airway. Immunity. 2015; 42:294–308. [PubMed: 25692703]

27. Hung LY, et al. IL-33 drives biphasic IL-13 production for noncanonical Type 2 immunity against hookworms. Proc Natl Acad Sci U S A. 2013; 110:282–287. [PubMed: 23248269]

28. Fallon PG, et al. Identification of an interleukin (IL)-25-dependent cell population that provides IL-4, IL-5, and IL-13 at the onset of helminth expulsion. J Exp Med. 2006; 203:1105–1116. [PubMed: 16606668]

29. Palm NW, et al. Bee venom phospholipase A2 induces a primary type 2 response that is dependent on the receptor ST2 and confers protective immunity. Immunity. 2013; 39:976–985. [PubMed: 24210353]

30. Matloubian M, et al. Lymphocyte egress from thymus and peripheral lymphoid organs is dependent on S1P receptor 1. Nature. 2004; 427:355–360. [PubMed: 14737169]

31. Gauvreau GM, et al. Effects of an anti-TSLP antibody on allergen-induced asthmatic responses. N Engl J Med. 2014; 370:2102–2110. [PubMed: 24846652]

32. Shih HY, et al. Developmental Acquisition of Regulomes Underlies Innate Lymphoid Cell Functionality. Cell. 2016; 165:1120–1133. [PubMed: 27156451]

33. Koues OI, et al. Distinct Gene Regulatory Pathways for Human Innate versus Adaptive Lymphoid Cells. Cell. 2016; 165:1134–1146. [PubMed: 27156452]

34. Robinette ML, et al. Transcriptional programs define molecular characteristics of innate lymphoid cell classes and subsets. Nat Immunol. 2015; 16:306–317. [PubMed: 25621825]

35. Guo L, et al. Innate immunological function of Th2 cells in vivo. Nat Immunol. 2015; 16:1051–1059. [PubMed: 26322482]

36. Neill DR, et al. Nuocytes represent a new innate effector leukocyte that mediates type-2 immunity. Nature. 2010; 464:1367–1370. [PubMed: 20200518]

37. Cortez VS, et al. Transforming Growth Factor-β Signaling Guides the Differentiation of Innate Lymphoid Cells in Salivary Glands. Immunity. 2016; 44:1127–1139. [PubMed: 27156386]

38. Gasteiger G, Fan X, Dikiy S, Lee SY, Rudensky AY. Tissue residency of innate lymphoid cells in lymphoid and nonlymphoid organs. Science. 2015; 350:981–985. [PubMed: 26472762]

39. Wakim LM, Woodward-Davis A, Bevan MJ. Memory T cells persisting within the brain after local infection show functional adaptations to their tissue of residence. Proc Natl Acad Sci U S A. 2010; 107:17872–17879. [PubMed: 20923878]

40. Thome JJ, et al. Spatial map of human T cell compartmentalization and maintenance over decades of life. Cell. 2014; 159:814–828. [PubMed: 25417158]

41. Steinert EM, et al. Quantifying Memory CD8T Cells Reveals Regionalization of Immunosurveillance. Cell. 2015; 161:737–749. [PubMed: 25957682]

42. von Moltke J, Locksley RM. I-L-C-2 it: type 2 immunity and group 2 innate lymphoid cells in homeostasis. Curr Opin Immunol. 2014; 31:58–65. [PubMed: 25458996]

METHODS-ONLY REFERENCES

43. Reese TA, et al. Chitin induces accumulation in tissue of innate immune cells associated with allergy. Nature. 2007; 447:92–96. [PubMed: 17450126]

44. Van Dyken SJ, et al. Fungal chitin from asthma-associated home environments induces eosinophilic lung infiltration. J Immunol. 2011; 187:2261–2267. [PubMed: 21824866]

45. Li H, Durbin R. Fast and accurate short read alignment with Burrows-Wheeler transform. Bioinformatics. 2009; 25:1754–1760. [PubMed: 19451168]

46. Quinlan AR, Hall IM. BEDTools: a flexible suite of utilities for comparing genomic features. Bioinformatics. 2010; 26:841–842. [PubMed: 20110278]

47. Picard Tools. 2015. <http://broadinstitute.github.io/picard/>

48. Zhang Y, et al. Model-based analysis of ChIP-Seq (MACS). Genome Biol. 2008; 9:R137. [PubMed: 18798982]

49. Langmead B, Salzberg SL. Fast gapped-read alignment with Bowtie 2. Nat Methods. 2012; 9:357–359. [PubMed: 22388286]

50. Trapnell C, Pachter L, Salzberg SL. TopHat: discovering splice junctions with RNA-Seq. Bioinformatics. 2009; 25:1105–1111. [PubMed: 19289445]

51. Flicek P, et al. Ensembl 2014. Nucleic Acids Res. 2014; 42:D749–D755. [PubMed: 24316576]

52. Anders S, Huber W. Differential expression analysis for sequence count data. Genome Biol. 2010; 11:R106. [PubMed: 20979621]
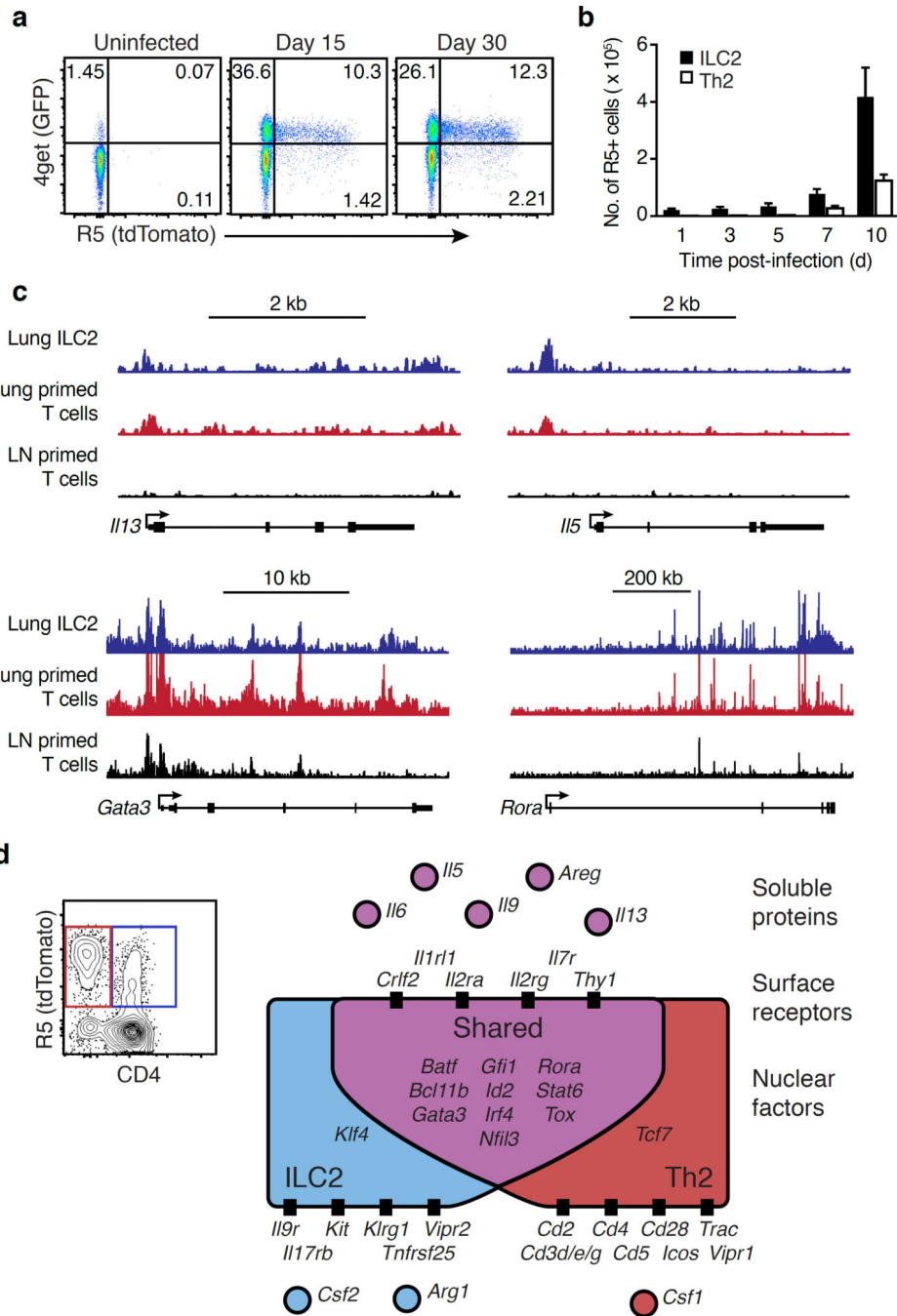
Fig. 1.

Cytokine reporters mark innate and adaptive tissue effectors. **a**, Flow cytometry of lung CD4$^+$ T cells from uninfected or *N. brasiliensis*-infected R5/4get dual reporter mice. **b**, R5$^+$ ILC2s and R5$^+$ CD4$^+$ T cells in lungs of mice on the indicated days of infection, presented as mean ± SEM. **c**, representative tracks pooled from ATAC-Seq reads aligning to *Il5*, *Il13*, *Gata3*, and *Rora*, shown with identical vertical scale. **d**, Representative flow cytometry of lung CD8$^-$CD19$^-$NK1.1$^+$CD90.2$^+$ cells and schematic Venn diagram of secreted proteins, cell surface markers, and nuclear factors that were significantly enriched in ILC2s (blue),

T$_H$2 cells (red), or shared without detection of statistical difference (purple). Data are (a) representative of 3 independent experiments; (b) pooled from 2 independent experiments for a total of at least 3 mice per time point; (c) from 2 (lung ILC2s), 3 (lung T cells), and 4 (LN T cells) biological replicates; (d) collected from 2 independent infections prior to sequencing for a total of 6 ILC2 and 5 T$_H$2 cell biological replicates.
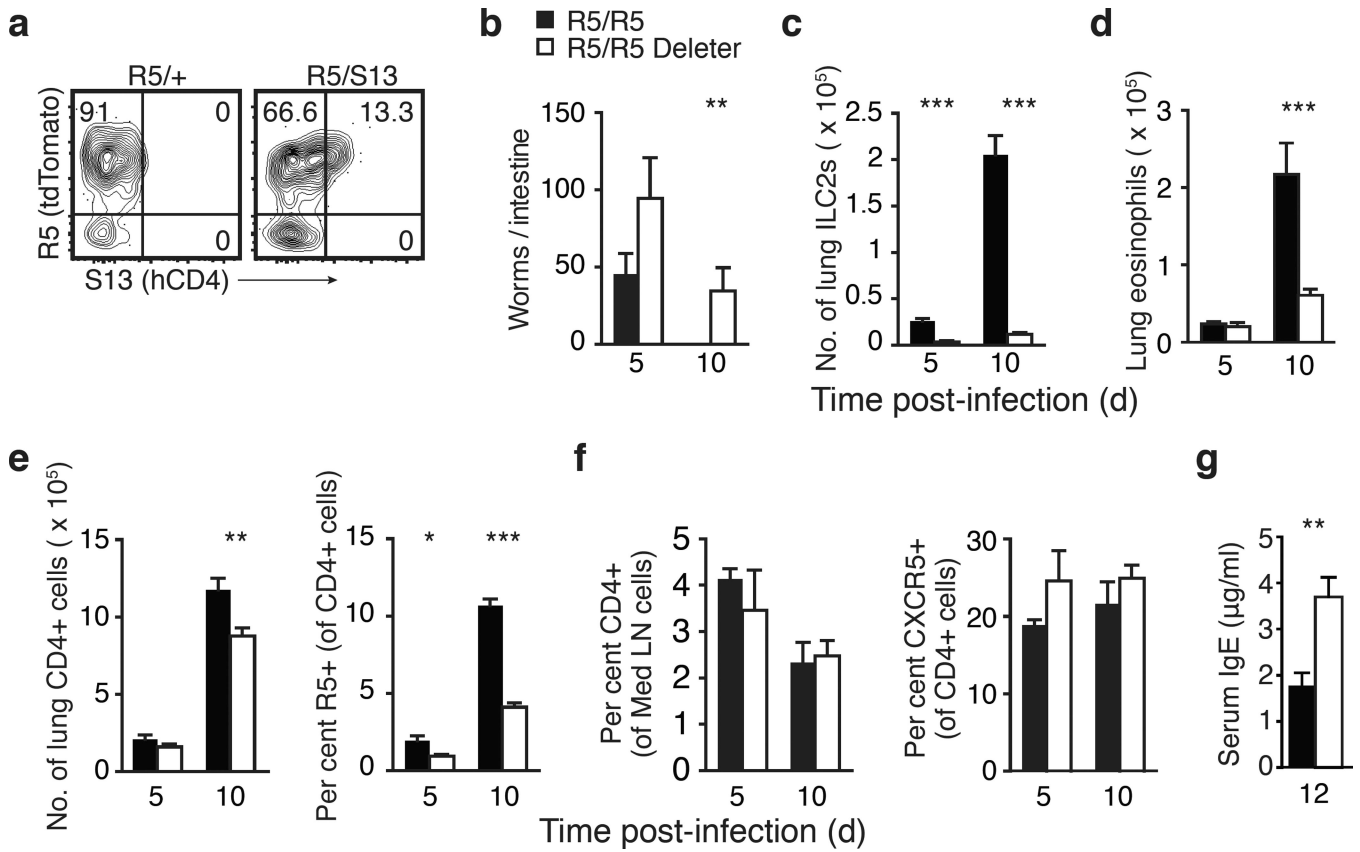
Fig. 2.
IL-5-producing cells drive type 2 immunity in the lung, but not the draining lymph node. **a**, Flow cytometry of lung ILC2s from R5/+ or R5/S13 mice 10 days post infection (d.p.i.) with *Nb* **b**, worm clearance, **c**, lung Lin⁻KLRG1⁺ ILC2s, **d**, lung eosinophils, **e**, lung CD4⁺ T cells and percent R5⁺ TH2 effector cells **f**, percent CD4⁺ T cells and PD-1⁺CXCR5⁺ TFH cells in the draining lymph nodes, and **g**, serum IgE in R5/R5 or R5/R5 Deleter mice on the indicated d.p.i. Data are (a) representative of 3 independent experiments, (b–e) pooled from 4 independent experiments for at least 5 mice per genotype, (f,g) pooled from 2 independent experiments for at least 5 mice per genotype. Lin, lineage; Med LN, mediastinal lymph node; TFH, T follicular helper cells; *, p < 0.05; **, p < 0.01; ***, p < 0.001.
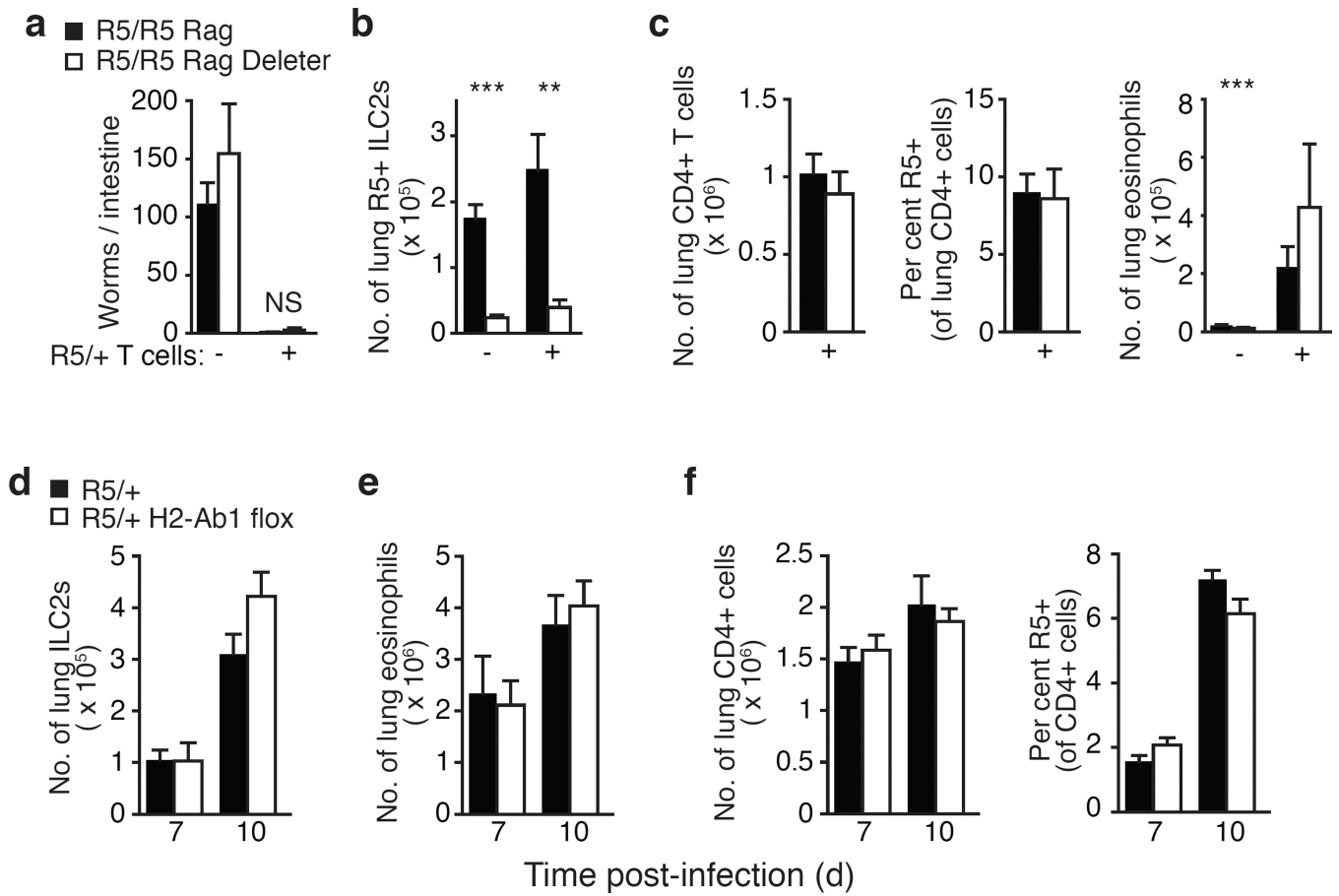
Fig 3.
Activation of adaptive type 2 immunity despite ILC2 deficiency. Rag1-deficient mice (either R5/R5 or R5/R5 Deleter) received no cells or naïve R5/+ CD4+ T cells and were analyzed 10 days post infection (d.p.i.) for **a**, worm counts, **b**, R5+ ILC2s, and **c**, CD4+ T cells, percent of T cells expressing R5, and lung eosinophils. **d**, Lin−Thy1+KLRG1+ ILC2s, **e**, eosinophils, and **f**, CD4+ T cells and R5+ TH2 effector cells in the lungs on the indicated d.p.i. Data are pooled from (a–c) 4 independent experiments for at least 5 mice per group or (d–e) 2 experiments for at least 3 mice per group. NS, not significant; *, $p < 0.05$; **, $p < 0.01$; ***, $p < 0.001$.
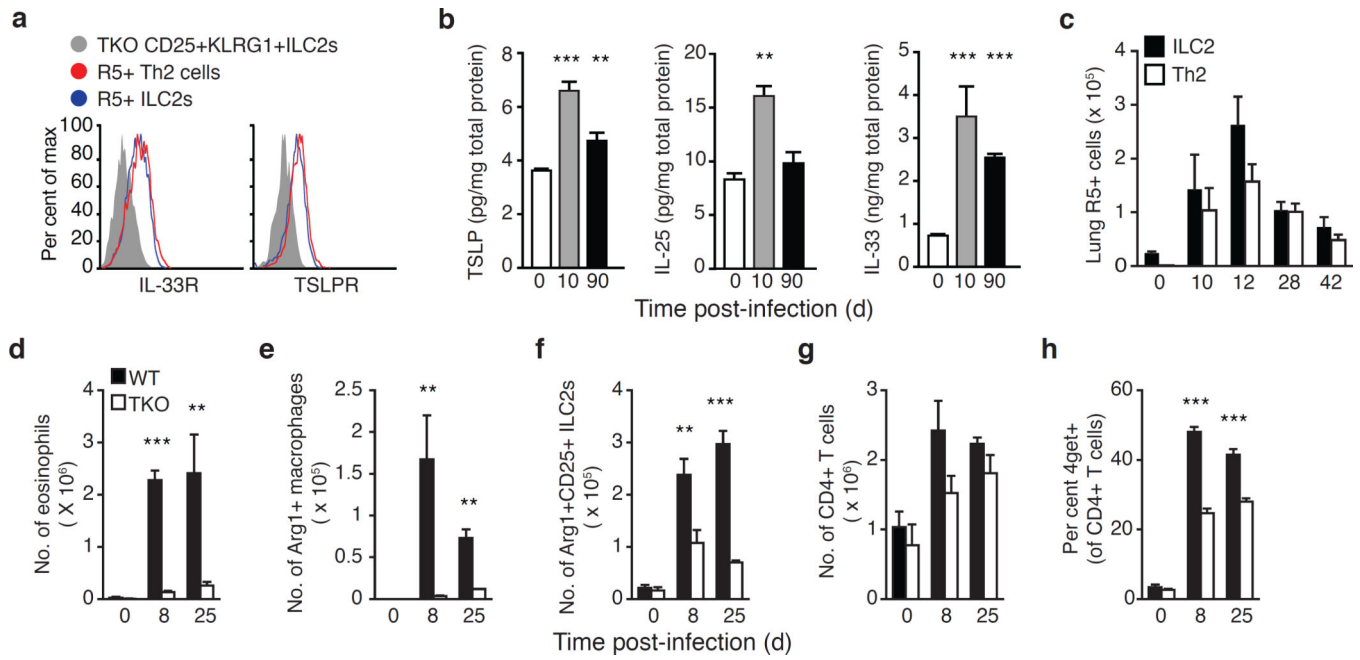
Fig. 4.
Multiple epithelial cytokines are induced in tissue during type 2 immunity. **a**, Histogram showing surface staining of IL-33 receptor and TSLP receptor on lung R5^{+} ILC2s (blue) and R5^{+} CD4^{+} T cells (red) 14 d.p.i. compared with lung ILC2s from a TKO mouse (gray). **b**, TSLP, IL-25, and IL-33 protein amounts in whole lung lysates from WT C57BL/6 mice at indicated days post *Nb* infection (d.p.i.). **c**, Number of R5^{+} ILC2s and R5^{+} CD4^{+} T cells in lungs of mice at the indicated d.p.i. **d**, Lung eosinophils, **e**, Arg1^{+} macrophages, and **f**, Arg1^{+}CD25^{+}ILC2s in BALB/c wild-type (WT) or *Crlf2^{-/-}Il25^{-/-}Il1rl1^{-/-}* triple-deficient (TKO) mice on Arg1 (Yarg) / IL4 (4get) dual reporter background. **g**, CD4^{+} T cells in 4get/Arg1 BALB/c (WT) or TKO lungs at indicated d.p.i. **h**, 4get^{+} cells as a percent of total lung CD4^{+} T cells. Data in (a) representative of 5 mice of each genotype from 2 independent experiments and in (b–h) pooled from 2 independent experiments for a total of at least 3 mice per group, represented as mean ± SEM, **, $p < 0.001$; ***, $p < 0.0001$.
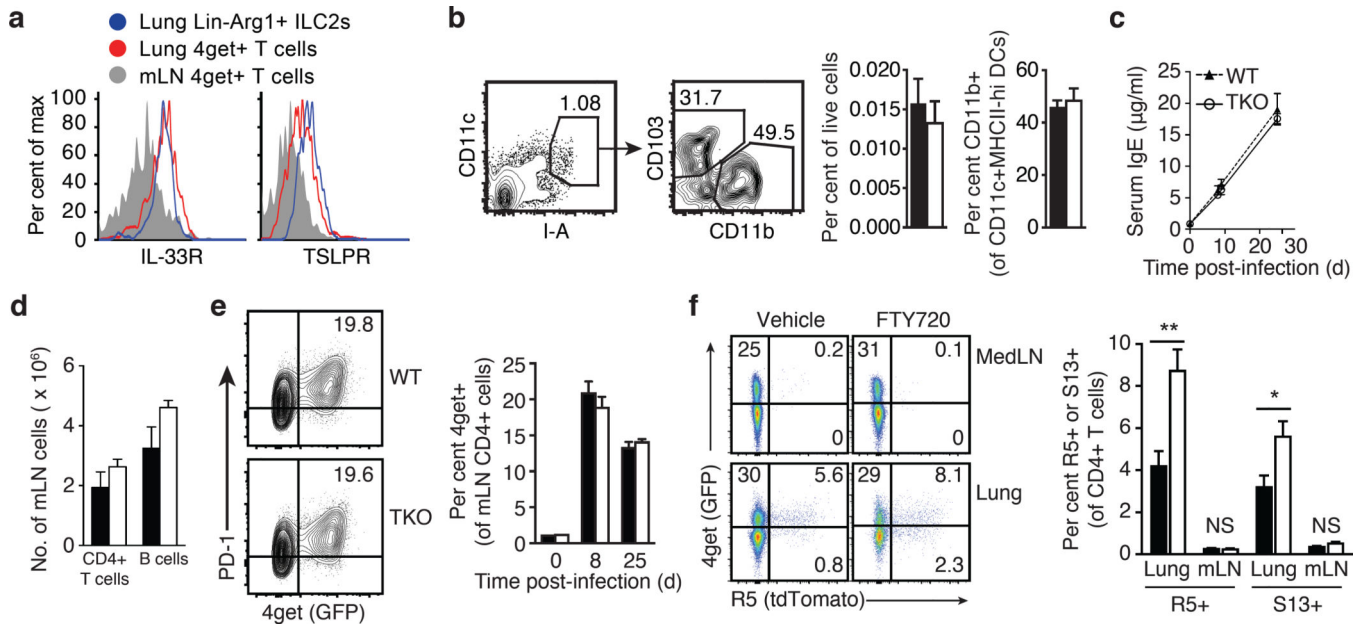
Fig. 5.
Tissue cytokines are not required for lymph node adaptive immunity. **a**, Histogram showing surface staining of IL-33 receptor and TSLP receptor on lung ILC2s (blue), lung 4get^{+} T cells (red), and mediastinal lymph node (mLN) 4get^{+} T cells (gray) 10 days post infection (d.p.i.). **b**, Representative flow cytometry and quantification of mLN CD11c^{+}MHCII^{hi} dendritic cells 3 d.p.i., previously gated on CD4^{−}CD8^{−}CD19^{−} cells. **c**, Serum IgE concentrations at indicated d.p.i. in WT and TKO mice. **d**, Numbers of CD4^{+} T cells, B cells, and **e**, percent of CD4^{+} T cells expressing T$_{FH}$ markers PD-1 and 4get in the mLN of indicated mice 8 d.p.i. **f**, Representative flow cytometry and quantification of the R5+ or S13+ percentage of CD4^{+} T cells in the lung and mLN of dual reporter mice 7 d.p.i that were treated with FTY720 or vehicle. Flow cytometric analysis in (a), (b), and (e) representative of 3 independent experiments, quantification in (b) and (f) representative of 2 independent experiments with at least 3 mice per group, and data in (c–e) pooled from 2 independent experiments for at least 3 mice per group, all presented as mean ± SEM, *, p < 0.05; **, p < 0.01; NS, no statistically significant difference.
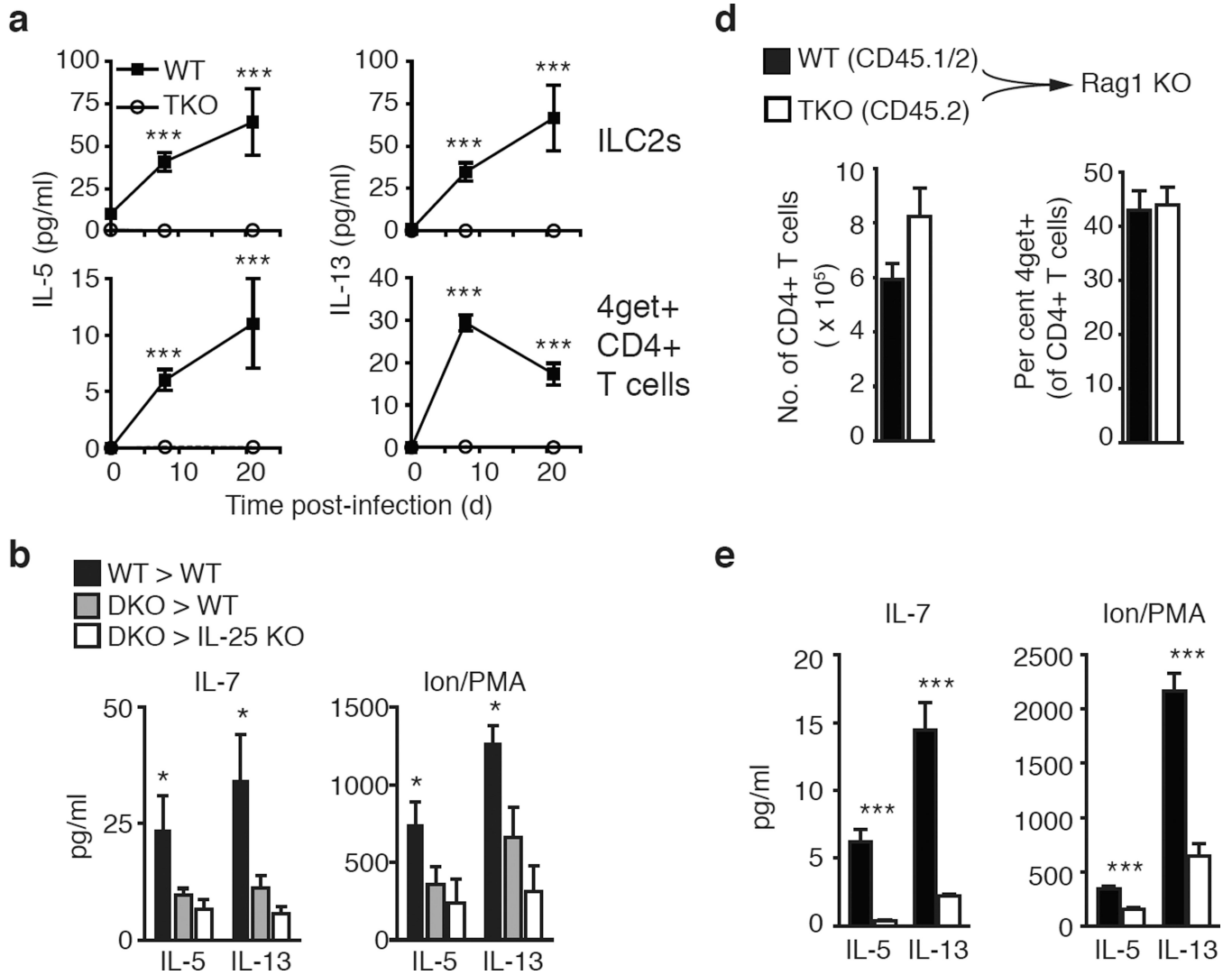
Fig. 6.
Tissue cytokine licensing of T_H2 cells is cell-intrinsic. **a**, IL-5 and IL-13 in supernatants of lung ILC2s or 4get⁺CD4⁺ T cells sorted at the indicated days post *Nb* infection (d.p.i.) and then cultured in IL-7 for 24 hours. **b**, IL-5 and IL-13 in supernatants of 24-hour IL-7 or Ion/PMA cultures of donor WT or IL-33R / TSLPR double-deficient (DKO) 4get⁺CD4⁺ T cells sorted from the lungs of WT or IL-25 KO recipients 10 d.p.i. **c**, Numbers of total donor-derived congenic WT and TKO CD4⁺ T cells and percentage 4get⁺ cells in the lungs of Rag1-deficient recipients and **d**, IL-5 and IL-13 in the supernatants of 24-hour IL-7 or Ion/PMA cultures of sorted lung 4get⁺CD4⁺ T cells 8 d.p.i. Data are presented as mean ± SEM, pooled from 2 independent experiments for at least 3 (a) and (b) or 6 (c) and (d) mice per group, represented as mean ± SEM. *, p < 0.05 in (b) refers to comparison between WT and similarly treated DKO cells; ***, p < 0.001.
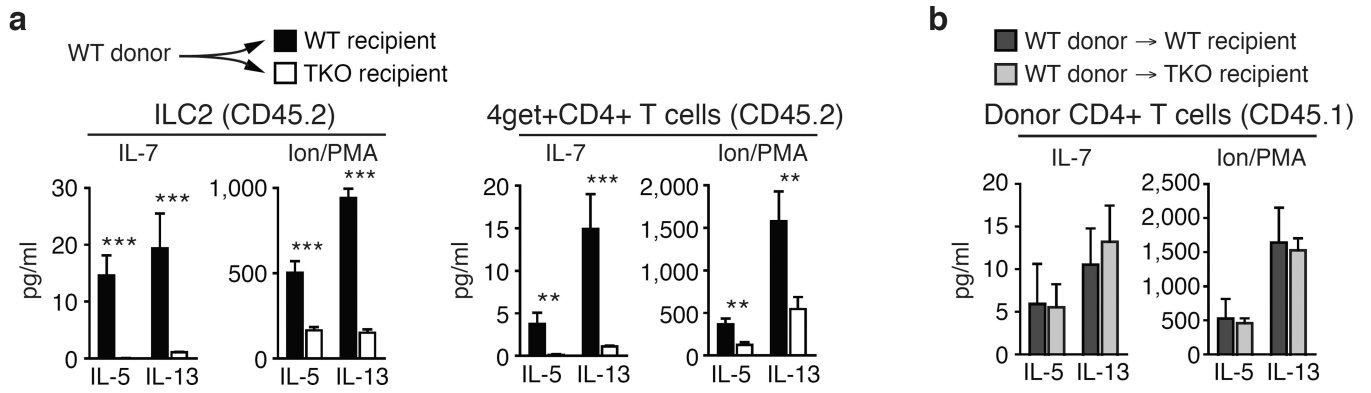
Fig. 7.
Cell-intrinsic epithelial cytokine signaling is sufficient for terminal TH2 cell differentiation. IL-5 and IL-13 in supernatant of 24-hour IL-7 or Ion/PMA cultures of **a**, recipient CD45.2+ ILC2s or 4get+CD4+ T cells sorted from WT or TKO CD45.2+ recipients or **b**, donor WT CD45.1+CD4+ T cells sorted from lungs of WT or TKO recipients 8 days after *Nb* infection. Data are presented as mean ± SEM and represent at least 3 mice per group pooled from 2 independent experiments; **, p < 0.01; ***, p < 0.001, compared to similarly-treated TKO.